

# Electropolymerization of polyaniline nanowires on poly(2-hydroxyethyl methacrylate) coated Platinum electrode

Maria Fernanda Xavier Pinto Medeiros<sup>1</sup>, Maria Elena Leyva<sup>1,2\*</sup> , Alvaro Antonio Alencar de Queiroz<sup>2</sup> and Liliam Becheran Maron<sup>3</sup>

<sup>1</sup>*Instituto de Físico Química, Universidade Federal de Itajubá – UNIFEI, Itajubá, MG, Brasil*

<sup>2</sup>*Laboratório de Alta Tensão, Universidade Federal de Itajubá – UNIFEI, Itajubá, MG, Brasil*

<sup>3</sup>*Instituto de Ciencia y Tecnología de Materiales, Universidad de la Habana – UH, Calle Zapata, Habana, Cuba*

\*[mariae@unifei.edu.br](mailto:mariae@unifei.edu.br)

## Abstract

A platinum electrode (Pt) was coated with poly(2-hydroxyethyl methacrylate) (PHEMA) by electrochemical polymerization using chronopotentiometry. Electropolymerization of polyaniline nanowires doped with camphorsulfonic acid (PANI:CSA) was further performed on the surface of the Pt-PHEMA electrode by cyclic voltammetry. The coated Pt-PHEMA-PANI:CSA electrode was characterized by Fourier transform infrared spectroscopy (FTIR), cyclic voltammetry (CV), electrochemical impedance spectroscopy (EIS), and scanning electron microscopy (SEM). According to EIS, the Pt-PHEMA electrode exhibits a charge transport resistance ( $R_{ct}$ ) of 169.19 k $\Omega$ . The EIS analysis of Pt-PHEMA-PANI:CSA electrode reveals a less resistive character ( $R_{ct}=1.28 \Omega$ ) than the observed for the Pt electrode coated with PANI:CSA ( $R_{ct}=0.47 \text{ k}\Omega$ ). As demonstrated by SEM, the Pt-PHEMA-PANI:CSA electrode has a high surface area due to the PANI:CSA nanowires embedded in Pt-PHEMA. The biocompatibility of PHEMA, allied to the electrochemical characteristics of PANI:CSA, could be useful to the development of implantable electrodes for biomedical applications.

**Keywords:** *electroactive hydrogels, chronopotentiometry, cyclic voltammetry, polyaniline, poly(2-hydroxyethyl methacrylate).*

**How to cite:** Medeiros, M. F. X. P., Leyva, M. E., Queiroz, A. A. A., & Maron, L. B. (2020). Electropolymerization of polyaniline nanowires on poly(2-hydroxyethyl methacrylate) coated Platinum electrode. *Polímeros: Ciência e Tecnologia*, 30(1), e2020008. <https://doi.org/10.1590/0104-1428.02020>

## 1. Introduction

There has been recently an increasing interest in the development of soft implantable microelectrodes for medicine<sup>[1-3]</sup>. The long-term implementation of this technology, however, has not yet been achieved due to practical issues that can be mainly related to the biological tissue response at the microelectrode interface<sup>[4-7]</sup>.

Electroconductive hydrogels (ECH) have shown significant potential for the design of implantable microelectrodes for medicine, bringing together the redox switching and the electrical properties of inherently conductive electroactive polymers with high hydration levels and biocompatibility properties, providing a soft and conductive interface<sup>[8-12]</sup>. When compared to conventional metal electrodes, implantable microelectrodes coated with ECH exhibit low interfacial impedance at the biological tissue interface and provide the necessary biocompatibility for long-term implantation<sup>[13-15]</sup>.

Several research groups have strategically explored the electrochemical synthesis (ECS) of poly(2-hydroxyethyl methacrylate) (PHEMA) from the monomer 2-hydroxyethyl methacrylate (HEMA) at metallic surfaces to reduce inflammatory reactions at the biological interface tissue-titanium<sup>[16,17]</sup>. At this interface, however, leachable chemicals from PHEMA, such

as catalysts, chemical initiators, and organic solvents, were shown to cause cytotoxicity, resulting in severe biological effects ranging from the alteration of cellular transduction pathways and gene expression levels to cell transformation, mutagenesis, and cell death<sup>[18,19]</sup>.

A key limitation for the preparation of effective implantable PHEMA microelectrodes capable of interfacing with living tissues and organs is related to the high resistance of this polymer. The incorporation of polymers containing a spatially extended  $\pi$  bonding system appears to represent a simple approach to overcome this limitation.

The combination of the conductive properties of polyaniline (PANI) with the hydrophilic nature of PHEMA makes PHEMA-PANI a dynamic and versatile ECH for biomedical purposes. The conductive emeraldine salt of PANI has attractive dedoping and redoping processes that increase conductivity, making it closer to that of metals or semiconductors, while offering an easy synthetic method and biocompatibility with biological tissues<sup>[20]</sup>.

It is well known that the conductivity of PANI can be adjusted by doping with secondary agents such as camphorsulfonic

acid (CSA)<sup>[21]</sup>. Additionally, PANI nanofibers are obtained during the electrochemical polymerization of aniline in the presence of camphorsulfonic acid (CSA)<sup>[22]</sup>. It is believed that CSA anions have a “surfactant-like” property that induces the formation of aggregates in solution which act as supramolecular-templates for fibrillary PANI growth<sup>[22]</sup>.

The present paper aims at the electropolymerization of PANI with fibrillary morphology by cyclic voltammetry and at its further embedding in PHEMA, synthesized through chronopotentiometric technique in an aqueous medium. The PHEMA-PANI microstructure was characterized by various analytical techniques such as Fourier transform infrared spectroscopy (FTIR) and scanning electron microscopy (SEM). Results on the electroactivity and electrical behavior of the PHEMA impregnated with fibrillary PANI molecules were respectively studied by cyclic voltammetry (CV) and electrochemical impedance spectroscopy (EIS).

## 2. Materials and Methods

### 2.1 Materials

Monomer 2-hydroxyethyl methacrylate (HEMA), potassium chloride (KCl), camphorsulfonic acid (CSA), hydrochloric acid (HCl), and dimethylformamide (DMF) were obtained from Sigma-Aldrich (Brazil) and used as received. Aniline was purchased from Sigma-Aldrich (Brazil) and purified by vacuum distillation at 70 °C. Other chemicals were also of analytical grade and used without any further purification.

### 2.2 Electrodeposition of PHEMA hydrogel on Pt electrode (Pt-PHEMA)

In the present study, the synthesis of PHEMA-PANI at the surface of platinum (Pt) electrodes was conducted in a two-step procedure. In the first step, PHEMA chains were electrodeposited at Pt electrodes (45.0 mm in length and 0.45 mm of diameter) by a chronopotentiometric technique using a Metrohm potentiostat/galvanostat model AUTOLAB PGSTAT302N (NOVA interface). The electrodeposition of PHEMA at the surface of Pt electrodes was conducted in an aqueous solution of 0.4 M HEMA monomer. The reactions were conducted at constant currents of 50, 125, and 200 mA for 1 hour at room temperature (25 °C) and air atmosphere. The PHEMA hydrogel polymerized on the Pt surface (Pt-PHEMA) was thoroughly washed with distilled water and dried under vacuum at 50 °C. The synthesis conditions for the first step were optimized to obtain PHEMA hydrogels with the best mechanical properties on the surface of Pt electrodes.

### 2.3 Electropolymerization of PANI on Pt-PHEMA electrode (Pt-PHEM-PANI:CSA)

In the second step, the Pt-PHEMA electrode was immersed in an aqueous solution of 0.5 M aniline containing 1.0 M CSA. The electropolymerization of PANI was performed at a Metrohm potentiostat/galvanostat, model AUTOLAB PGSTAT302N (NOVA interface), via cyclic voltammetry in the potential range of 1.4 to 0.05 V and scan rate of 50 mV/s. The Pt-PHEMA was used as the working electrode, a platinum wire as the counter electrode, and Ag/AgCl as the reference

electrode. After the reaction, the Pt-PHEMA-PANI:CSA was thoroughly washed with distilled water and dried in a vacuum oven at 50 °C until constant weight.

### 2.4 Characterizations

Morphologies of Pt-PHEMA and Pt-PHEMA-PANI:CSA were studied by scanning electron microscopy (SEM). SEM micrographs of the samples were performed using a scanning electron microscopy (Carl Zeiss Model EVO MA 15). The samples were previously coated with gold and analyzed using an applied tension of 10 to 15 kV.

The microstructure of the PHEMA-PANI at the Pt interface was recorded in the range of 650–4000 cm<sup>-1</sup> by Fourier transform infrared spectroscopy (FTIR) in a Perkin Elmer Spectrum 100 FTIR spectrometer equipped with an attenuated total reflectance accessory (ATR) and resolution of 4 cm<sup>-1</sup>.

Electrochemical characterization of Pt-PHEMA-PANI:CSA electrodes was performed using a Metrohm Autolab PGSTAT302N potentiostat/galvanostat controlled by the NOVA software. The Pt-PHEMA and Pt-PHEMA-PANI:CSA were used as working electrodes, Pt wire as the counter electrode, and Ag/AgCl as the reference electrode. The electrochemical behavior of Pt-PHEMA and Pt-PHEMA-PANI:CSA was studied by cyclic voltammetry from -0.2 to 1.0 V, at a scan rate of 50 mV/s considering 3 cycles.

The electrochemical impedance spectra of the samples were obtained potentiostatically; the AC signal was recorded in the frequency range from 0.1 to 103 Hz, and the DC potential was set to 0 V and used as input. Both cyclic voltammetry and electrochemical impedance spectroscopy (EIS) measurements were carried out in an aqueous solution of 1.0 M HCl. The electrochemical cell was kept in air atmosphere and at 25 °C during all experiments.

## 3. Results and Discussions

### 3.1 Chronopotentiometry deposition of PHEMA at Pt surface

The polymerization of HEMA at Pt surface is an example of a free radical reaction in which water molecules undergo electrolysis to form hydroxyl radicals (HO<sup>•</sup>). The HO<sup>•</sup> radicals serve as initiators for the electropolymerization process by generating free radicals on the >C=C< bonds of HEMA<sup>[23-25]</sup>. During the propagation step, the crosslinking of PHEMA appears to form chains in a 3D framework due to the functional nature of HEMA monomers.

In this work, chronopotentiometric electrolysis of HEMA on Pt electrodes, at different applied currents, was investigated to search for the adequate hydrogen evolution (from water electrolysis) that allowed increasing the PHEMA coating thickness at the Pt surface. Figure 1 shows the potential waveform responses at different applied currents. The experimental results (Figure 1) suggest that HEMA can be reduced at the cathode prior to the hydrogen reduction. An organic deposit was rapidly formed at the cathodic surface after reduction of the monomer. The deposit appears to have low conductivity and causes a significant decrease in the

electrolytic current (Figure 1). It was found that PHEMA is formed in appreciable yield at the Pt surface.

For comparison, PANI was also electrosynthesized using CSA at the surface of the Pt electrode in an aqueous medium. Figure 2 shows the cyclic voltammograms recorded during 14 cycles for the electropolymerization of PANI:CSA on the Pt electrode surface. The deposition of oxidized aniline starts from the first cycle at 0.9 V (Figure 2, peak B); in later cycles, the oxidation potential is seen at peak A (Figure 2, 0.34 V), suggesting the formation of a low-molecular-mass cation radical. The cathodic peak (A\*) is observed at 0.19 V. This A-A\* redox couple corresponds to the redox pernigraniline-emeraldine process<sup>[26]</sup>.

### 3.2 Electropolymerization of embedded PANI:CSA in Pt-PHEMA

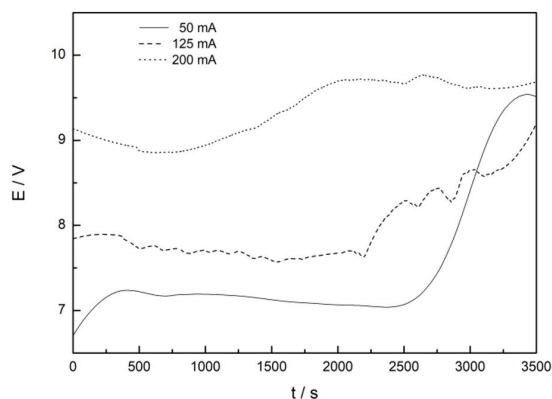
Incorporation of PANI:CSA into the framework of Pt-PHEMA is primarily driven by the osmotic pressure present across PHEMA on the Pt electrode surface and by the dipole-dipole interactions between CSA and carbonyl oxygen, giving an amphiphilic nature to PHEMA at the Pt electrode surface. Thus, during the electropolymerization process, PANI:CSA spreads into the interior and external surfaces of Pt-PHEMA to form a channel for ionic conduction. The ionic conduction channel suggests a “bottom-up” approach, in which nanowire PANI structures are built up from aniline molecules by self-assembly.

Figure 3 shows the cyclic voltammogram recorded during the electropolymerization of PANI:CSA embedded in Pt-PHEMA electrode. The oxidation of aniline starts from the first cycle at 0.9V but at a lower anodic current (1.4mA) if compared to that of aniline oxidized directly on the Pt electrode (3.2 mA, Figure 2). This difference can be explained considering that oxidation is directly proportional to the concentration of monomers next to the Pt-PHEMA electrode surface.

Therefore, the diffusion of aniline through hydrogel in Pt-PHEMA decreases the monomer concentrations next to the electrode surface. It can be seen that the oxidation of aniline is also significant in the second cycle (Figure 3). The second cycle shows the oxidation of cation-radicals at peak A (0.33 V), that exhibits a potential shift to more positive values during the electropolymerization process. The cathodic peak (A\*, Figure 3) is observed at 0.19 V. The A-A\* redox couple pernigraniline-emeraldine was observed at the same potential during the electropolymerization of PANI:CSA on Pt electrode. The only difference is seen at the lower current of both cathodic and anodic peaks (Figure 3). This observation could be due to the reduction in the aniline concentration that diffuses through Pt-PHEMA.

### 3.3 Structural analysis

FTIR-ATR spectroscopy was used to characterize the chemical structure of Pt-PHEMA, Pt-PANI:CSA, and Pt-PHEMA-PANI:CSA. Figure 4 shows the FTIR spectra of Pt-PHEMA. The absorption bands at 1163  $\text{cm}^{-1}$  (C-O stretch), 1500-1350  $\text{cm}^{-1}$  (C-H bend), 1731  $\text{cm}^{-1}$  (C=O stretch), 2976  $\text{cm}^{-1}$  (C-H stretch), and 3459  $\text{cm}^{-1}$  (O-H stretch) are in good agreement with those given in previous works of



**Figure 1.** Potential waveform responses at 50 mA, 125 mA, and 200 mA vs. time for the chronopotentiometric deposition of PHEMA at Pt electrodes.

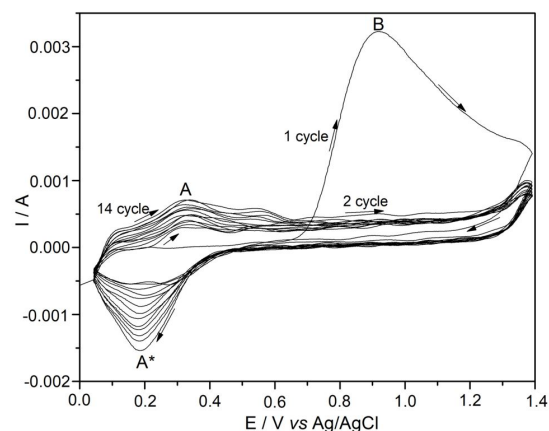


**Figure 2.** Cyclic voltammograms of electrochemical polymerization of aniline on Pt electrode in aqueous solution of 0.5 M aniline containing CSA at 1.0 M, in the potential range of 0.05 to 1.4 V, scan rate of 50 mV/s, and room temperature (25 °C). A – A\* redox couple corresponds to pernigraniline – emeraldine process.

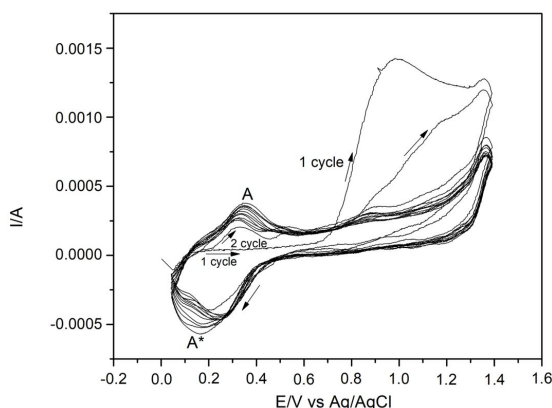


**Figure 3.** Cyclic voltammograms of the growth of PANI:CSA on Pt-PHEMA electrode in aqueous solution of 0.5 M aniline containing CSA at 1.0 M, scan rate of 50mV/s, and scan limits from 0.05V to 1.4V. A – A\* redox couple corresponds to the redox pernigraniline-emeraldine process.

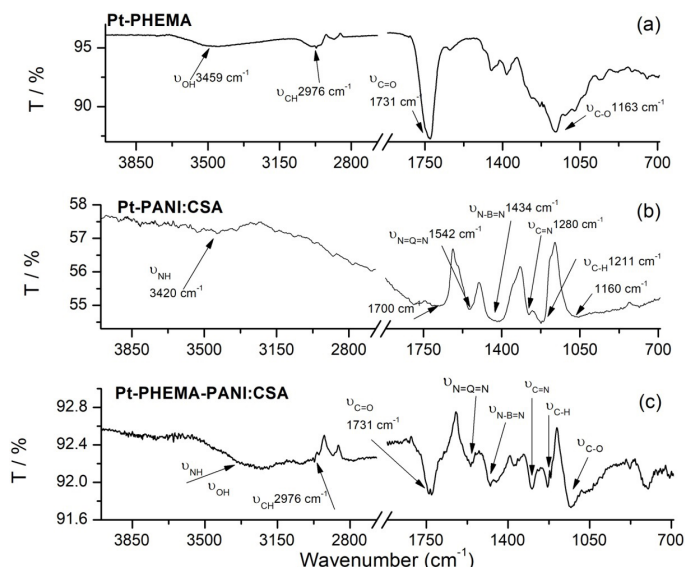


**Figure 4.** FTIR spectra of Pt-PHEMA (a), Pt-PANI:CSA (b) and Pt-PHEMA-PANI:CSA (c).

PHEMA, confirming the presence of a thin layer of PHEMA at Pt electrode surface<sup>[27]</sup>.

Figure 4b shows the FTIR spectra of Pt-PANI:CSA. The FTIR spectra show characteristic bands at 1700 cm<sup>-1</sup> and 1160 cm<sup>-1</sup> corresponding to the C=O and S=O stretching vibration, respectively. These bands confirm the presence of the camphorsulfonic acid and are in good consistency with the literature<sup>[28]</sup>. The quinoid and benzenoid absorption bands of PANI are seen at 1542 cm<sup>-1</sup> and 1434 cm<sup>-1</sup>, respectively. Characteristic absorption bands of PANI were also observed (Figure 4b) at 1280 cm<sup>-1</sup>, attributed to C=N stretching of secondary amines. The characteristic bands observed in the FTIR spectra of electrodeposited PANI:CSA at the Pt electrode surface are in good agreement with the literature<sup>[29]</sup>. The FTIR spectra of Pt-PHEMA-PANI:CSA (Figure 4c) did not present significant changes in the PHEMA or PANI FTIR-spectra, suggesting that PANI:CSA nanowires could be dispersed in-situ in Pt-PHEMA electrode.

The SEM micrographs of the Pt-PHEMA, Pt-PANI:CSA, and Pt-PHEMA-PANI:CSA can be observed in Figure 5. Morphology of Pt-PHEMA (Figure 5a) consists essentially of porous microstructures formed by aggregate granules of different shapes in the size of microns.

SEM micrographs of the Pt-PANI:CSA can be observed in Figure 5b. Morphology of PANI:CSA at Pt surface (Figure 5b) consists essentially of a heterogeneous microstructure formed by spheroidal granules in the range of microns alternating with fibrillary layers of PANI. Granules are organized in homogeneously distributed aggregates. The granular aggregates observed at the Pt-PANI:CSA surface suggest a characteristic morphological feature of PANI:CSA with a heterogeneous nucleation mechanism. The nanowire morphology of Pt-PHEMA-PANI:CSA can be clearly seen in Figure 5c. These images depict that PANI:CSA has a strong effect on the Pt-PHEMA morphology. The PANI:CSA nanowires embedded in Pt-PHEMA were found to have average diameters of 40-60 nm. Although the growth of PANI

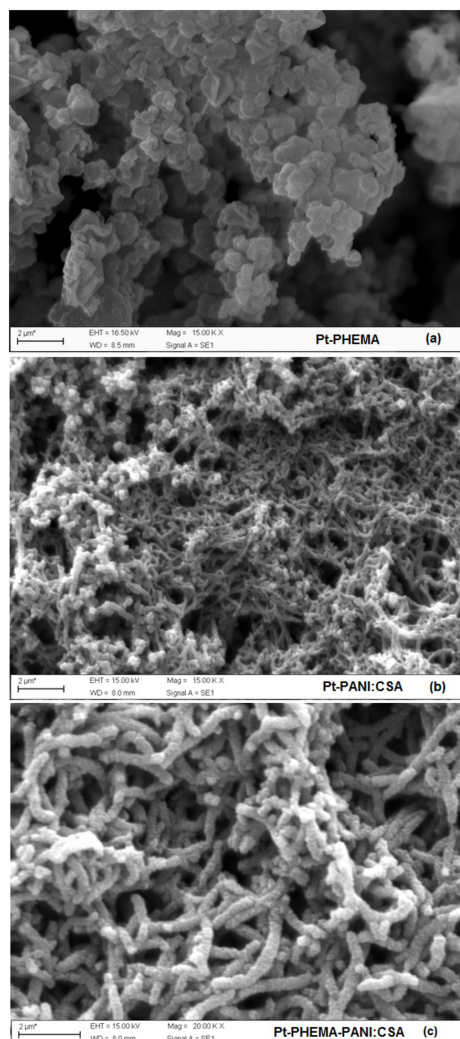


**Figure 5.** SEM micrographs of Pt-PHEMA (a), Pt-PANI:CSA (b) and Pt-PHEMA-PANI:CSA (c) electrodes surfaces.

nanowires has no directional alignment, the fibrils are uniform, suggesting a growth by diffusion of aniline at the Pt-PHEMA interface into a less-dense aqueous phase containing the CSA doping acid.

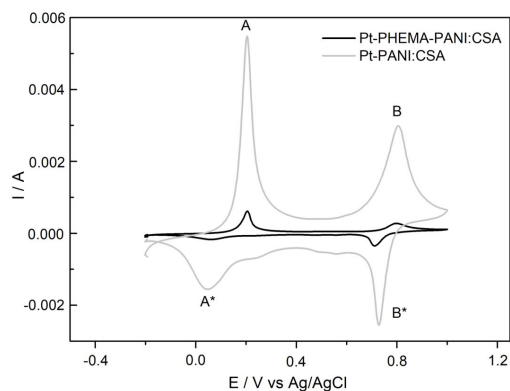
### 3.4 Electrical and electrochemical behaviors

Figure 6 shows the cyclic voltammetry (CV) curves of the modified Pt electrodes in the potential range of the two redox stages characteristic of polyaniline. The same redox couples were observed for both Pt-PANI:CSA and Pt-PHEMA-PANI:CSA electrodes. The first one (A\*/A) was observed at lower potential values (0.05V/0.20V) and may be associated with the transition leucoemeraldine/emeraldine. The second redox pair (B\*/B) presented higher potentials values (0.73V/0.8V) and was associated with the transition emeraldine/pernigraniline. These two redox couples show a behavior similar to the observed in polyaniline films prepared by aniline electropolymerization in an aqueous solution containing inorganic acids<sup>[30]</sup>. CV of Pt-PHEMA-PANI:CSA confirmed that the hydrogel maintains the electroactive properties of pure PANI:CSA. It was found that the electrical conductivity of the Pt-PHEMA electrode was enhanced after the growth of PANI:CSA nanowires (Pt-PHEMA-PANI).

To further understand the electron transfer resistance at the electrode/electrolyte interface, analyses of electrochemical impedance spectroscopy (EIS) were performed on Pt-PHEMA, Pt-PANI:CSA, and Pt-PHEMA-PANI:CSA. Nyquist plots obtained from EIS measurements are exhibited in Figure 7.

The observed semicircle indicates that the electron transfer at the surface of the electrode is a kinetically controlled process<sup>[28]</sup>. The diameter of the semicircle gives the resistance to the charge transfer ( $R_{ct}$ ) at the electrode surface. This resistance controls the kinetics of the electron transfer at the interface electrode/electrolyte<sup>[29]</sup>. The  $R_{ct}$  for Pt-PHEMA was 169.19 k $\Omega$  and indicates that PHEMA hinders the charge transfer at the Pt electrode surface. After modifying the Pt electrode with PANI:CSA, the  $R_{ct}$  decreased to 0.47 k $\Omega$ .; while, when PANI:CSA nanowires were growth in Pt-PHEMA, the  $R_{ct}$  dramatically decreased to 1.28  $\Omega$ , which indicates that PANI:CSA plays a role similar to a conductive Pt wire and thus makes electron transfer easier. The differences of  $R_{ct}$  among Pt-PHEMA, Pt-PANI:CSA, and Pt-PHEMA-PANI:CSA indicate that the electroactive PHEMA-PANI:CSA hydrogel has been effectively attached on the Pt surface. Lower CPE capacitances were obtained for the PANI film on Pt electrode, which might be due to a thick PHEMA film formed at the Pt electrode surface (0.54  $\mu$ F) if compared to Pt-PHEMA-PANI:CSA (9.54  $\mu$ F) and Pt-PANI:CSA (95.66  $\mu$ F). The drop in the capacitance of Pt-PHEMA-PANI:CSA relatively to Pt-PANI:CSA appears to be related with the higher ionic diffusion in the microporous surface of Pt-PHEMA-PANI:CSA caused by the presence of larger pores, which lead to a decrease of active sites on the electrode surface.

## 4. Conclusions



**Figure 6.** Cyclic voltammograms (CVs) of Pt-PANI:CSA and Pt-PHEMA-PANI:CSA in 1.0 M HCl aqueous solution at 20mV/s (from -0.2 V to 1.0 V). A - A\* redox couple corresponds to emeraldine - leucoemeraldine process, B - B\* redox couple corresponds to pernigraniline - emeraldine process.

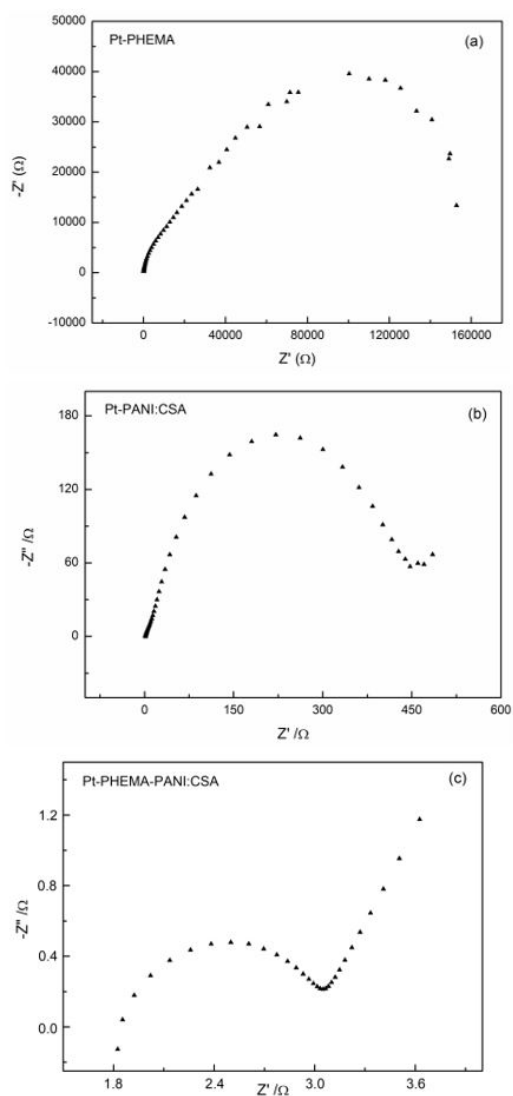


**Figure 7.** Nyquist diagrams for pHEMA-Pt (a), PANI.CSA-Pt (b) and PANI.CSA/pHEMA-Pt (c) in 1.0 M of HCl at frequency range 10 kHz - 100 MHz.

In the present study PHEMA, PANI:CSA, and PHEMA-PANI:CSA were successfully synthesized by employing chronoamperometric and cyclic voltammetry techniques on Pt electrodes and characterized by FTIR, cyclic voltammetry, electrochemical impedance spectroscopy, and SEM. FTIR results showed that PHEMA can be efficiently electropolymerized by chronopotentiometry on the Pt electrode. In such conditions, Pt-PHEMA showed high values of  $R_{ct}$  resistance, exhibiting a highly porous structure. The PANI:CSA electropolymerized on Pt electrode presented a heterogeneous morphology formed by a dense network. EIS analyses showed a low  $R_{ct}$  resistance in PANI:CSA-Pt. The Pt-PHEMA-PANI:CSA showed a less resistive character (lower  $R_{ct}$ ) than PANI:CSA. The cyclic voltammetry results indicate that Pt-PHEMA-PANI:CSA keeps the electroactive character of Pt-PANI:CSA.

## 5. Acknowledgements

We would like to acknowledge the Fundação de Amparo à Pesquisa do Estado de Minas Gerais (FAPEMIG), Conselho Nacional de Desenvolvimento Científico e Tecnológico (CNPq), Coordenação de Aperfeiçoamento de Pessoal de Ensino Superior (CAPES), for the financial support of this project.

## 6. References

- Chung, A. J., Kim, D., & Erickson, D. (2008). Electrokinetic microfluidic devices for rapid, low power drug delivery in autonomous microsystems. *Lab on a Chip*, 8(2), 330-338. <http://dx.doi.org/10.1039/B713325A>. PMID:18231674.
- Abidian, M. R., & Martin, C. D. (2009). Neural interface biomaterials: multifunctional nanobiomaterials for neural interfaces. *Advanced Functional Materials*, 19(4), 573-585. <http://dx.doi.org/10.1002/adfm.200801473>.
- Muller, R., Yue, Z., Ahmadi, S., Ng, W., Grosse, W. M., Cook, M. J., Wallace, G. G., & Moulton, S. E. (2016). Development and validation of a seizure initiated drug delivery system for the treatment of epilepsy. *Sensors and Actuators. B, Chemical*, 236, 732-740. <http://dx.doi.org/10.1016/j.snb.2016.06.038>.
- Kim, D.-H., Abidian, M. R., & Martin, D. C. (2004). Conducting polymers grown in hydrogel scaffolds coated on neural prosthetic devices. *Journal of Biomedical Materials Research. Part A*, 71(4), 577-585. <http://dx.doi.org/10.1002/jbma.30124>. PMID:15514937.
- Green, R. A., Lovell, H. N., Wallace, G. G., & Poole-Warren, A. L. (2008). Conducting polymers for neural interfaces: challenges in developing an effective long-term implant. *Biomaterials*, 29(24-25), 3393-3399. <http://dx.doi.org/10.1016/j.biomaterials.2008.04.047>. PMID:18501423.
- Abidian, M. R., Corey, J. M., Kipke, D. R., & Martin, D. C. (2010). Conducting-polymer nanotubes improve electrical properties, mechanical adhesion, neural attachment, and neurite outgrowth of neural electrodes. *Small*, 6(3), 421-429. <http://dx.doi.org/10.1002/sml.200901868>. PMID:20077424.
- He, L., Lin, D., Wang, Y., Xiao, Y., & Che, J. (2011). Electroactive SWNT/PEGDA hybrid hydrogel coating for bio-electrode interface. *Colloids and Surfaces. B, Biointerfaces*, 87(2), 273-279. <http://dx.doi.org/10.1016/j.colsurfb.2011.05.028>. PMID:21676598.
- Brahim, S., & Guiseppi-Elie, A. (2005). Electroconductive Hydrogels: Electrical and Electrochemical Properties of Polypyrrole-Poly(HEMA) composites. *Electroanalysis*, 17(7), 556-570. <http://dx.doi.org/10.1002/elan.200403109>.
- Guiseppi-Elie, A. (2010). Electroconductive hydrogels: synthesis, characterization and biomedical applications. *Biomaterials*, 31(10), 2701-2716. <http://dx.doi.org/10.1016/j.biomaterials.2009.12.052>. PMID:20060580.
- Guo, B., Finne-Wistrand, A., & Albertsson, A. C. (2011). Degradable and Electroactive Hydrogels with Tunable Electrical Conductivity and Swelling Behavior. *Chemistry of Materials*, 23(5), 1254-1262. <http://dx.doi.org/10.1021/cm103498s>.
- Kotanen, C. N., Wilson, A. N., Dong, C., Dinu, C. Z., Justin, G. A., & Guiseppi-Elie, A. (2013). The effect of the physicochemical properties of bioactive electroconductive hydrogels on the growth and proliferation of attachment dependent cells. *Biomaterials*, 34(27), 6318-6327. <http://dx.doi.org/10.1016/j.biomaterials.2013.05.022>. PMID:23755835.
- Pérez-Martínez, C. J., Morales Chávez, S. D., del Castillo-Castro, T., Lara Ceniceros, T. E., Castillo-Ortega, M. M., Rodríguez-Félix, D. E., & Gálvez Ruiz, J. C. (2016). Electroconductive nanocomposite hydrogel for pulsatile drug release. *Reactive & Functional Polymers*, 100, 12-17. <http://dx.doi.org/10.1016/j.reactfunctpolym.2015.12.017>.
- Schwartz, A. B. (2004). Cortical neural prosthetics. *Annual Review of Neuroscience*, 27(1), 487-507. <http://dx.doi.org/10.1146/annurev.neuro.27.070203.144233>. PMID:15217341.
- Polikov, V. S., Tresco, A. P., & Reichert, M. W. (2005). Response of brain tissue to chronically implanted neural electrodes. *Journal of Neuroscience Methods*, 148(1), 1-18. <http://dx.doi.org/10.1016/j.jneumeth.2005.08.015>. PMID:16198003.
- Xie, K., Wang, S., Aziz, T. Z., Stein, J. F., & Liu, X. (2006). The physiologically modulated electrode potentials at the depth electrode-brain interface in humans. *Neuroscience Letters*, 402(3), 238-243. <http://dx.doi.org/10.1016/j.neulet.2006.04.015>. PMID:16697525.
- Prashantha, K., Vasanta, K., Pai, K., & Shergira, B. S. (2002). Electrochemical synthesis of poly[2-Hydroxyethylmethacrylate] hydrogel: kinetics and mechanism. *Journal of Applied Polymer Science*, 84(5), 983-992. <http://dx.doi.org/10.1002/app.10299>.
- De Giglio, E., Cometa, S., Ricci, M. A., Cafagna, D., Savino, A. M., Sabbatini, L., Orciani, M., Ceci, E., Novello, L., Tantillo, G. M., & Mattioli-Belmonte, M. (2011). Ciprofloxacin-modified electrosynthesized hydrogel coatings to prevent titanium-implant-associated infections. *Acta Biomaterialia*, 7(2), 882-891. <http://dx.doi.org/10.1016/j.actbio.2010.07.030>. PMID:20659594.
- De Giglio, E., Cometa, S., Satriano, C., Sabbatini, L., & Zamboni, P. G. (2009). Electrosynthesis of hydrogel films on metal substrates for the development of coatings with tunable drug delivery performances. *Journal of Biomedical Materials Research. Part A*, 88(4), 1048-1057. <http://dx.doi.org/10.1002/jbma.31908>. PMID:18404708.
- De Giglio, E., Cafagna, D., Giangregorio, M. M., Domingos, M., Mattioli-Belmonte, M., & Cometa, S. (2011). PHEMA-based thin hydrogel films for biomedical applications. *Journal of Bioactive and Compatible Polymers*, 26(4), 420-434. <http://dx.doi.org/10.1177/0883911511410460>.
- Humpolicek, P., Kasparkova, V., Saha, P., & Stejskal, J. (2012). Biocompatibility of polyaniline. *Synthetic Metals*, 162(7-8), 722-727. <http://dx.doi.org/10.1016/j.synthmet.2012.02.024>.
- Xia, Y., Wiesinger, J. M., MacDiarmid, A. G., & Epstein, A. J. (1995). Camphorsulfonic acid fully doped polyaniline emeraldine salt: conformations in different solvents studied by an ultraviolet/visible/near-infrared spectroscopic method. *Chemistry of Materials*, 7(5), 443-445. <http://dx.doi.org/10.1021/cm00051a002>.

22. Zhang, X., & Manohar, S. K. (2004). Polyaniline nanofibers: chemical synthesis using surfactants. *Chemical Communications*, 2004(20), 2360-2361. <http://dx.doi.org/10.1039/b409309g>. PMID:15490020.
23. Baute, N., Martinot, L., & Jérôme, R. (1999). Investigation of the cathodic electropolymerization of acrylonitrile, ethylacrylate and methylmethacrylate by coupled quartz crystal microbalance analysis and cyclic voltammetry. *Journal of Electroanalytical Chemistry*, 472(1), 83-90. [http://dx.doi.org/10.1016/S0022-0728\(99\)00275-2](http://dx.doi.org/10.1016/S0022-0728(99)00275-2).
24. Decker, C., Vataj, R., & Louati, A. (2004). Synthesis of acrylic polymer networks by electroinitiated polymerization. *Progress in Organic Coatings*, 50(4), 263-268. <http://dx.doi.org/10.1016/j.porgcoat.2004.03.005>.
25. De Giglio, E., Cometa, S., Cioffi, N., Torsi, L., & Sabbatini, L. (2007). Analytical investigations of poly(acrylic acid) coatings electrodeposited on titanium-based implants: a versatile approach to biocompatibility enhancement. *Analytical and Bioanalytical Chemistry*, 389(7-8), 2055-2063. <http://dx.doi.org/10.1007/s00216-007-1299-7>. PMID:17516054.
26. Babaiee, M., Pakshir, M., & Hashemi, B. (2015). Effects of potentiodynamic electropolymerization parameters on electrochemical properties and morphology of fabricated PANI nanofiber/graphite electrode. *Synthetic Metals*, 199, 110-120. <http://dx.doi.org/10.1016/j.synthmet.2014.11.012>.
27. Ali, N., Duan, X., Jiang, Z.-T., Goh, B. M., Lamb, R., Tadich, A., Poinern, G. E. J., Fawcett, D., Chapman, P., & Singh, P. (2014). Surface and interface analysis of poly-hydroxyethylmethacrylate-coated anodic aluminium oxide membranes. *Applied Surface Science*, 289, 560-563. <http://dx.doi.org/10.1016/j.apsusc.2013.11.042>.
28. Namazi, H., Kabiri, R., & Entezami, A. (2002). Determination of extremely low percolation threshold electroactivity of the blend polyvinyl chloride/polyaniline doped with camphorsulfonic acid by cyclic voltammetry method. *European Polymer Journal*, 38(4), 771-777. [http://dx.doi.org/10.1016/S0014-3057\(01\)00232-4](http://dx.doi.org/10.1016/S0014-3057(01)00232-4).
29. Pruneanu, S., Veress, E., Marian, I., & Oniciu, L. (1999). Characterization of polyaniline by cyclic voltammetry and UV-Vis absorption spectroscopy. *Journal of Materials Science*, 34(11), 2733-2739. <http://dx.doi.org/10.1023/A:1004641908718>.
30. Vyas, R. N., & Wang, B. (2010). Electrochemical analysis of conducting polymer thin films. *International Journal of Molecular Sciences*, 11(4), 1956-1972. <http://dx.doi.org/10.3390/ijms11041956>. PMID:20480052.

Received: Feb. 13, 2020

Revised: Apr. 24, 2020

Accepted: Apr. 29, 2020